

Supplemental Information for:

Evidence for a Kinetically Controlled Burying Mechanism for Growth of High Viscosity
Secondary Organic Aerosol

Allison C. Vander Wall, Véronique Perraud, Lisa M. Wingen, and Barbara J. Finlayson-Pitts*

Department of Chemistry

University of California

Irvine, CA, 92697-2025

Environmental Science: Processes & Impacts

*Corresponding author: Email: bjfinlay@uci.edu; phone: (949) 824-7670; FAX: (949) 824-2420

AMS ratio of NO^+ and NO_2^+

Because of extensive fragmentation of the parent ions in the AMS, organic nitrates were measured using the peak intensities of the NO^+ and NO_2^+ fragments. However, these fragments can also be generated from inorganic nitrates and nitric acid which could be formed by decomposition of the organic nitrates. Since these experiments were carried out at low relative humidity, hydrolysis is unlikely and thermal decomposition at room temperature is also not expected to be significant. However, to establish that the signals are consistent with organic nitrates, the ratio of NO^+ to NO_2^+ for all three organic nitrates, either with or without CH, was measured. Table S1 shows this ratio was between 3.1 and 5.4 for all of the organic nitrates used here (there was no statistical difference between 7 and 31 min reaction time). These values are consistent with the ratios for organic nitrates measured in other systems,¹⁻³ and differ significantly from that of nitric acid (Table S1).^{4,5} These ratios suggest that the nitrate that is taken up into the particles remains an intact organic nitrate. This is also supported by the lack of detectable peaks around 1350 cm^{-1} due to inorganic NO_3^- in the infrared spectra (Figure S1).

Table S1: HR-ToF-AMS ratio of NO^+ to NO_2^+ for particles formed in the presence of 1.4×10^{14} 2EHN molecules cm^{-3} , 1.2×10^{14} HPN molecules cm^{-3} , and 5.0×10^{12} HHN molecules cm^{-3} , either with or without the OH scavenger CH (Series C). For comparison, that for nitric acid is also given.

		Ratio^a of NO^+ to NO_2^+	
		No CH	With CH
Organic Nitrate	2EHN	5.4 ± 0.3	4.9 ± 1.6
	HPN	3.4 ± 0.3	3.1 ± 0.2
	HHN	4.6 ± 0.2	3.6 ± 0.4
Nitric Acid^{4,5}		0.33 - 0.86	

^aError bars are $\pm 2\sigma$ from the average of three experiments for the organic nitrates.

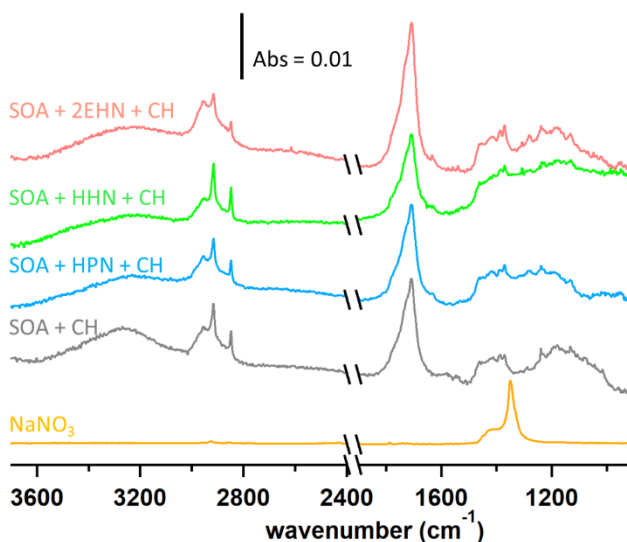
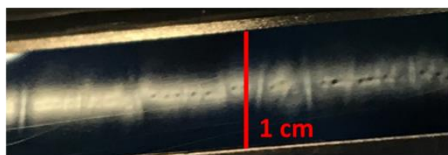
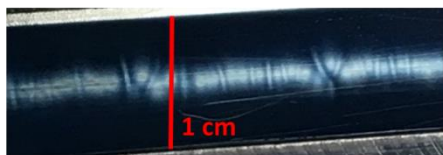


Figure S1: ATR-FTIR spectra for impacted particles alone, and particles formed in the presence of 2EHN, HPN or HHN in the flow reactor with CH as an OH scavenger (Series D). Also shown is the spectrum for $10 \mu\text{L}$ of a 0.52 M solution of NaNO_3 deposited on the crystal with the solvent subsequently evaporated. The NaNO_3 spectrum has been multiplied by a factor of 0.1. The region between $2500 - 2000 \text{ cm}^{-1}$ is not shown due to variations in the CO_2 (g) in the sampling compartment.

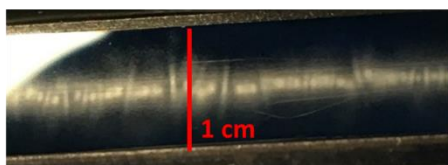
(a) SOA alone



(b) SOA formed with OH scavenger



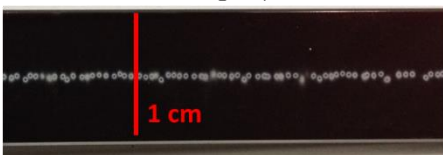
(c) SOA formed in the presence of HPN



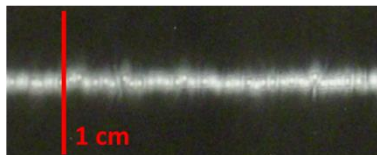
(d) SOA formed in the presence of HPN and OH scavenger



(e) Deliquesced Na_2SO_4 particles



(f) Dry carboxylate-modified latex particles



(g) SOA formed at 87% relative humidity

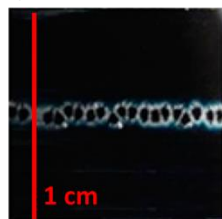


Figure S2: Typical impaction patterns for a) SOA alone for Series A without organic nitrate or CH, b) SOA formed in Series A in the presence of CH, c) SOA formed in the presence of HPN in the flow reactor (Series C/D), d) SOA formed in the presence of both HPN and CH (Series C/D), e) deliquesced Na_2SO_4 particles, f) dry 270 nm carboxylate-modified latex particles, and g) SOA particles formed at 87% relative humidity (parts e-g adapted from Kidd *et al.*).⁶

Table S2: AMS elemental analysis for SOA formed without organic nitrates either with or without 100 ppm of CH as an OH scavenger (Series C) at 31 min reaction time. The oxidation state of carbon (OS_c) is determined by $2(O:C) - H:C$.⁷

	SOA ^a	SOA + CH ^a
O:C	0.51 ± 0.02	0.48 ± 0.01
H:C	1.6 ± 0.01	1.6 ± 0.01
OS_c	-0.58 ± 0.05	-0.64 ± 0.03

^aError bars are $\pm 2\sigma$

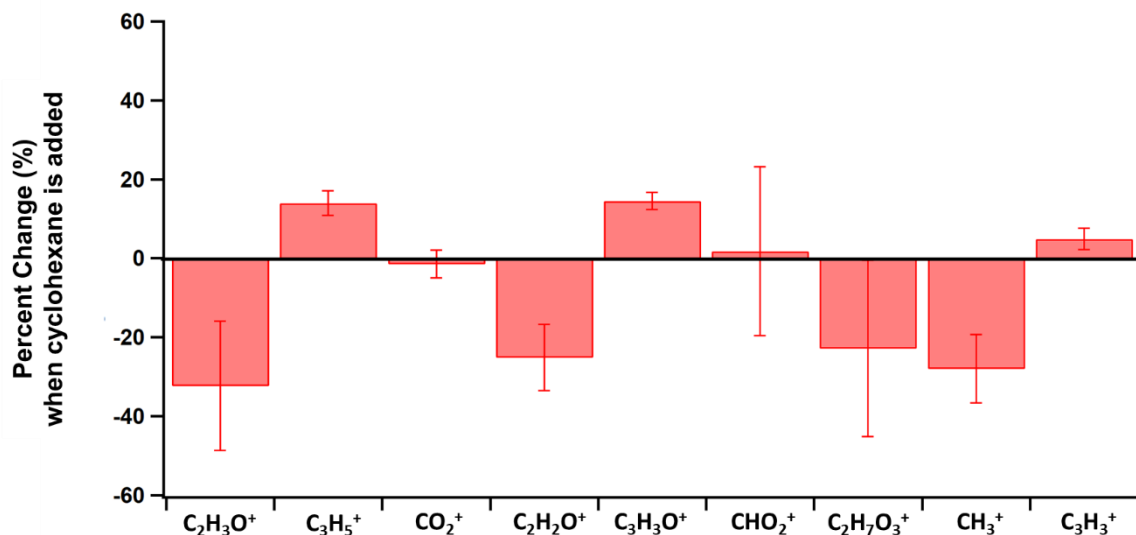


Figure S3: Percent change of some of the major fragments observed in the AMS spectra when CH is present compared to SOA formed without CH at 31 min reaction time. All fragments have been divided by HR_{Org} to account for differences in the total mass loading. Negative values indicate that the fragment is less abundant when the OH is scavenged, while positive values indicate that the fragment is more abundant when the OH is scavenged. Error bars are $\pm 2\sigma$ from the average of three experiments.

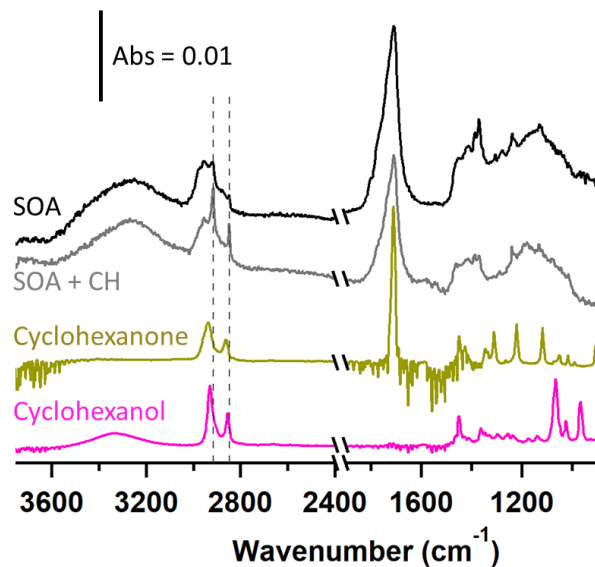


Figure S4: ATR-FTIR spectra for impacted SOA particles alone and SOA particles formed with CH as an OH scavenger. Also shown are the spectra for liquid cyclohexanone and cyclohexanol. The cyclohexanone and cyclohexanol spectra have been scaled by a factor of 0.1. The region between 2500 – 2000 cm⁻¹ is not shown due to variations in the CO₂ in the sampling compartment. The dashed lines at 2915 and 2850 cm⁻¹ are guides for the eye.

Table S3: Simplified reaction mechanism.

Reaction	k (cm ³ molecule ⁻¹ s ⁻¹) ^{8,9}
AP + O ₃ → OH + RO ₂ ^a	7.0 × 10 ⁻¹⁷
AP + O ₃ → Product1 ^a	1.7 × 10 ⁻¹⁷
AP + OH → RO ₂	5.4 × 10 ⁻¹¹
CH + OH → Products	7.2 × 10 ⁻¹²
Calculated from Group Contribution ¹⁰	
2EHN + OH → Products	6.3 × 10 ⁻¹²
HPN + OH → Products	1.3 ^b × 10 ⁻¹² <u>2.1^c × 10⁻¹²</u> Average ^d = (1.6 ± 0.5) × 10 ⁻¹²
HHN + OH → Products	4.2 ^b × 10 ⁻¹² <u>6.4^c × 10⁻¹²</u> Average ^d = (5.1 ± 1.3) × 10 ⁻¹²

^a 80% of AP + O₃ gives OH radicals,¹¹⁻¹³ and 20% of AP + O₃ gives low volatility products capable of forming particles (all products lumped together as Product1). The total AP + O₃ rate constant is 8.7 × 10⁻¹⁷.^{8,9}

^bHydroxy-terminated isomer

^cNitrate-terminated isomer

^dRate constants for HPN and HHN are weighted averages using the relative amounts of the two isomers. Error bars are ±1σ.

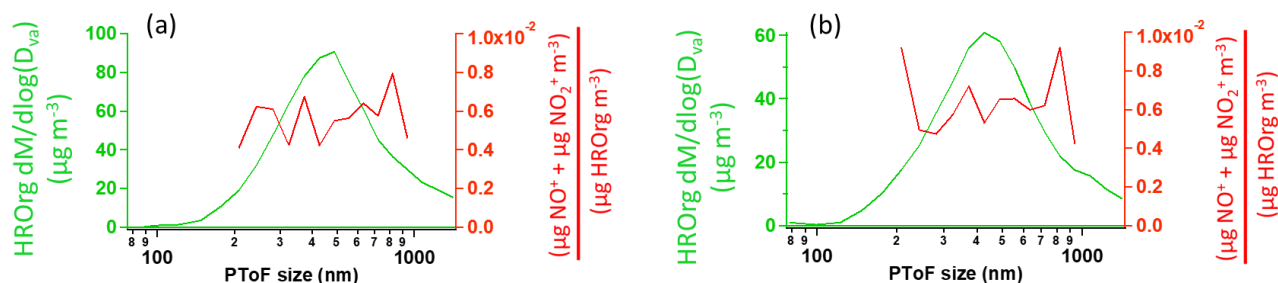


Figure S5: HR-PToF mass distribution of total HROrg (green) and the HR-PToF mass ratio of ($\text{NO}^+ + \text{NO}_2^+$) to HROrg (red) for a) SOA formed in the presence of HPN (1.2×10^{14} molecules cm^{-3}) at 7 min reaction time, and b) SOA formed in the presence of HPN and CH (2.5×10^{15} molecules cm^{-3}) at 7 min reaction time. Note the NO^+ and NO_2^+ signals in the presence of CH have high uncertainty due to weak signal.

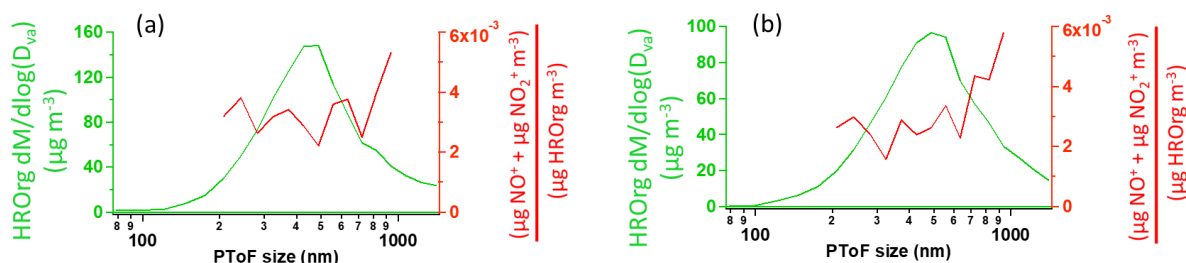


Figure S6: HR-PToF mass distribution of total HROrg (green) and the HR-PToF mass ratio of ($\text{NO}^+ + \text{NO}_2^+$) to HROrg (red) for a) SOA formed in the presence of HHN (5.0×10^{12} molecules cm^{-3}) at 7 min reaction time, and b) SOA formed in the presence of HHN and CH (2.5×10^{15} molecules cm^{-3}) at 7 min reaction time. Note the NO^+ and NO_2^+ signals in the presence of CH have high uncertainty due to weak signal.

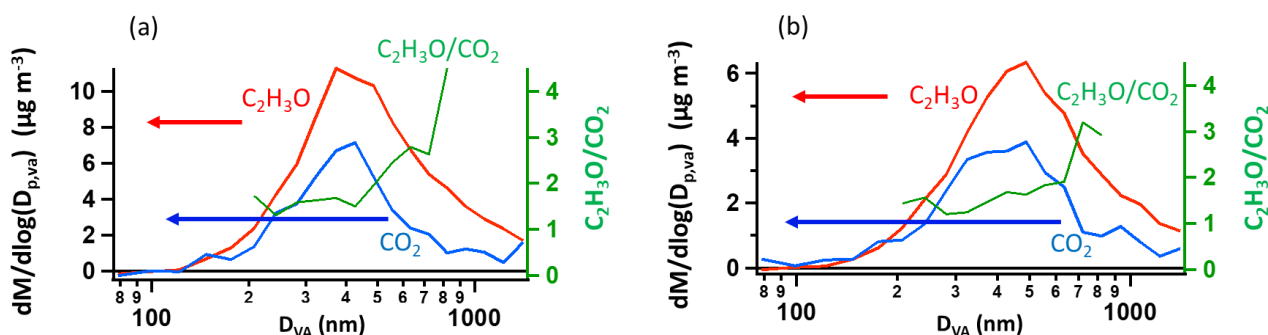


Figure S7: The HR-PToF mass distribution $\text{C}_2\text{H}_3\text{O}^+$ (red), CO_2^+ (blue), and the ratio of $\text{C}_2\text{H}_3\text{O}^+/\text{CO}_2^+$ (green) for a) SOA alone at 7 minutes reaction time, and b) SOA formed in the presence of CH (2.5×10^{15} molecules cm^{-3}) at 7 minutes reaction time.

References

1. E. A. Bruns, V. Perraud, A. Zelenyuk, M. J. Ezell, S. N. Johnson, Y. Yu, D. Imre, B. J. Finlayson-Pitts and M. L. Alexander, Comparison of FTIR and particle mass spectrometry for the measurement of particulate organic nitrates, *Environ. Sci. Technol.*, 2010, **44**, 1056-1061.
2. D. K. Farmer, A. Matsunaga, K. S. Docherty, J. D. Surratt, J. H. Seinfeld, P. J. Ziemann and J. L. Jimenez, Response of an aerosol mass spectrometer to organonitrates and organosulfates and implications for atmospheric chemistry, *Proc. Natl. Acad. Sci. U.S.A.*, 2010, **107**, 6670-6675.
3. A. W. Rollins, J. L. Fry, J. F. Hunter, J. H. Kroll, D. R. Worsnop, S. W. Singaram and R. C. Cohen, Elemental analysis of aerosol organic nitrates with electron ionization high-resolution mass spectrometry, *Atmos. Meas. Tech.*, 2010, **3**, 301-310.
4. C. S. S. O'Connor, N. C. Jones and S. D. Price, Electron-impact ionization of nitric acid, *Int. J. Mass Spectrom. Ion Process.*, 1997, **163**, 131-139.
5. R. A. Friedel, J. L. Shultz and A. G. Sharkey, Mass spectrum of nitric acid, *Anal. Chem.*, 1959, **31**, 1128-1128.
6. C. Kidd, V. Perraud, L. M. Wingen and B. J. Finlayson-Pitts, Integrating phase and composition of secondary organic aerosol from the ozonolysis of alpha-pinene, *Proc. Natl. Acad. Sci. U.S.A.*, 2014, **111**, 7552-7557.
7. J. H. Kroll, N. M. Donahue, J. L. Jimenez, S. H. Kessler, M. R. Canagaratna, K. R. Wilson, K. E. Altieri, L. R. Mazzoleni, A. S. Wozniak, H. Bluhm, E. R. Mysak, J. D. Smith, C. E. Kolb and D. R. Worsnop, Carbon oxidation state as a metric for describing the chemistry of atmospheric organic aerosol, *Nature Chem.*, 2011, **3**, 133-139.
8. B. J. Finlayson-Pitts and J. N. Pitts, *Chemistry of the Upper and Lower Atmosphere: Theory, Experiments, and Applications*, Academic Press, 2000.
9. R. Atkinson, Gas-phase tropospheric chemistry of volatile organic compounds: 1. Alkanes and alkenes, *J. Phys. Chem. Ref. Data*, 1997, **26**, 215-290.
10. E. S. C. Kwok and R. Atkinson, Estimation of hydroxyl radical reaction rate constants for gas-phase organic compounds using a structure-reactivity relationship: An update, *Atmos. Environ.*, 1995, **29**, 1685-1695.
11. R. Atkinson, S. M. Aschmann, J. Arey and B. Shorees, Formation of OH radicals in the gas phase reactions of O₃ with a series of terpenes, *J. Geophys. Res. Atmos.*, 1992, **97**, 6065-6073.
12. S. E. Paulson, M. Chung, A. D. Sen and G. Orzechowska, Measurement of OH radical formation from the reaction of ozone with several biogenic alkenes, *J. Geophys. Res. Atmos.*, 1998, **103**, 25533-25539.
13. C. D. Forester and J. R. Wells, Hydroxyl radical yields from reactions of terpene mixtures with ozone, *Indoor Air*, 2011, **21**, 400-409.